

Supporting Information

One-pot microwave synthesis of Pd modified titanium dioxide nanocrystals for 3D aerogel monoliths with efficient visible-light photocatalytic activity in a heated gas flow reactor

Junggou Kwon^a, Kyoungjun Choi^b, Elena Tervoort^a, and Markus Niederberger^{a*}

^a *Laboratory for Multifunctional Materials, Department of Materials, ETH Zurich, Vladimir-Prelog-Weg 5, 8093 Zürich, Switzerland*

^b *Institute for Chemistry and Bioanalytics, School of Life Sciences, FHNW University of Applied Sciences and Arts Northwestern, Hofackerstrasse 30, 4132 Muttenz, Switzerland*

*Email: markus.niederberger@mat.ethz.ch

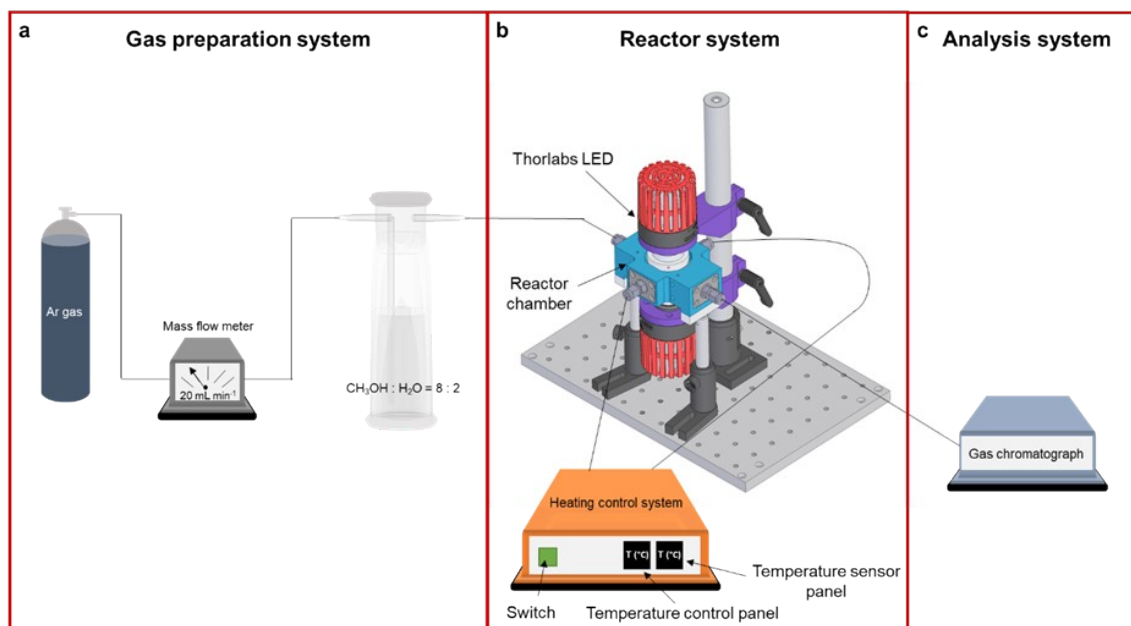


Figure S1.

Scheme of the complete Q-master reactor system consisting of (a) gas-preparation system with flow meter and liquid reactants, (b) reactor system with sample chamber, LEDs, and heater, and (c) analysis system composed of a gas chromatograph.

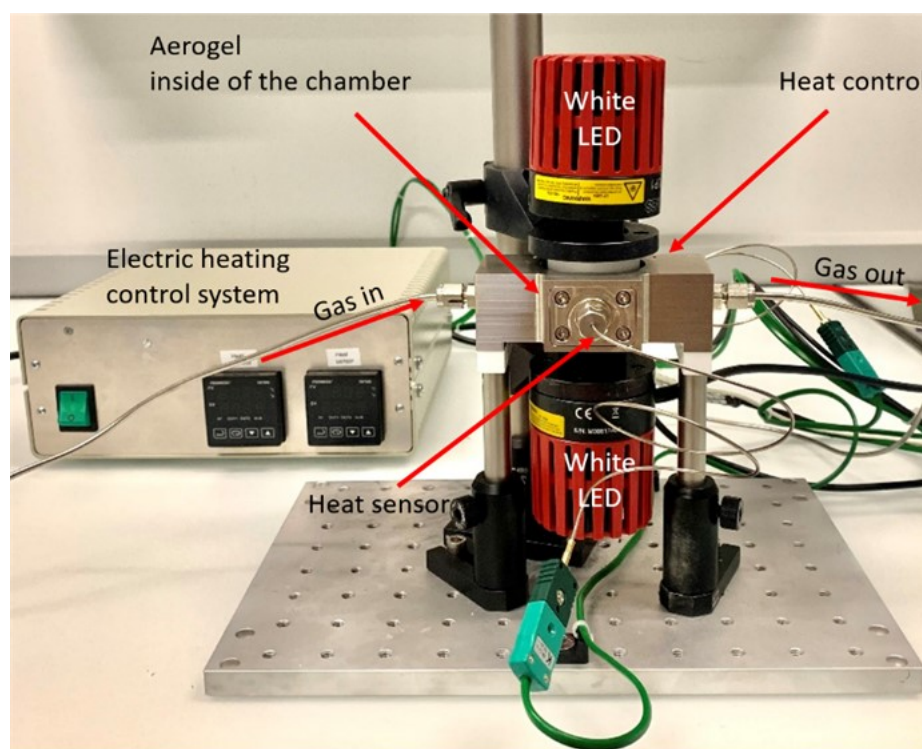
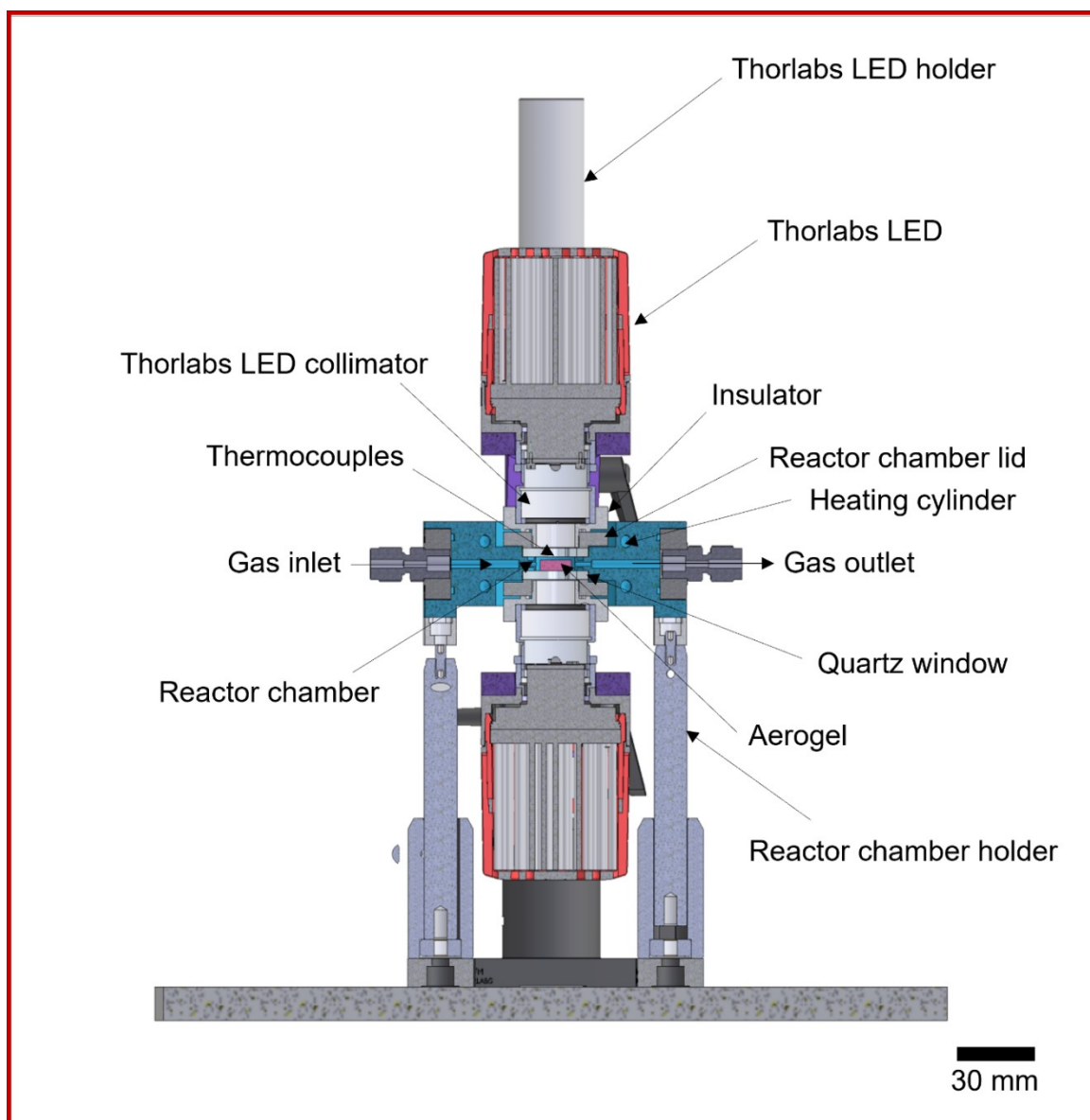


Figure S2. Digital photograph of the reactor system with sample chamber, LEDs, and heater.



Fig

Figure S3. Technical drawing of the Q-master reactor system with labeled components.

The monolithic aerogel pellet is loaded on the quartz window in the reactor chamber and oriented perpendicular to the light source (Thorlabs LEDs). The reactor chamber has a disk-like shape with a diameter of 15 mm and a height of 5 mm (total volume = 883.6 mm³). The chamber is closed by placing another quartz window and the reactor chamber lid made of stainless steel on the top. The chamber is sealed with six screws to prevent gas leakage. The gas inlet and outlet are designed to guide the gas along the cross-section of the aerogel. Four

heating cylinders made of heat-resistant chromium-nickel steel are placed inside the reactor chamber and connected to the heating control system. The temperature is measured by two thermocouples (type K). They are not shown in the image but placed near the aerogel. The first thermocouple is responsible for measuring the temperature of the gas in the chamber. The second thermocouple is for double checking the overheating of the chamber. The temperatures measured by the two thermocouples can be monitored in the temperature control panel and temperature sensor panel, respectively, in the heating control system.

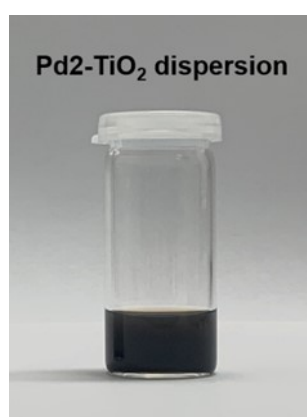


Figure S4. Digital photograph of Pd2-TiO₂ nanoparticle dispersion.

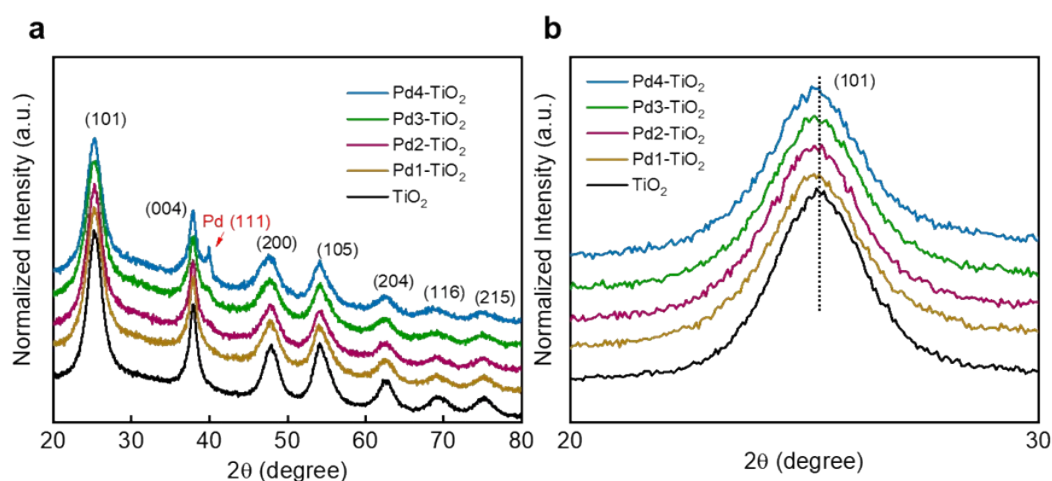


Figure S5. (a) XRD patterns of powdered TiO₂, Pd1-TiO₂, Pd2-TiO₂, Pd3-TiO₂, and Pd4-TiO₂ aerogels before annealing at 150 °C. (b) Magnification of the (101) XRD reflection of the TiO₂, Pd1-TiO₂, Pd2-TiO₂, Pd3-TiO₂, and Pd4-TiO₂ aerogels after annealing.

Sample	Crystallite size (nm)	Surface area (m ² g ⁻¹)	Pore volume (cm ³ g ⁻¹)
TiO ₂	6.9	433.2	1.892
Pd1-TiO ₂	6.1	422.7	1.422
Pd2-TiO ₂	5.8	420.7	1.395
Pd3-TiO ₂	5.8	416.5	1.352
Pd4-TiO ₂	6.2	387.0	1.265

Table S1. Crystallite size, surface area, and pore volume of the TiO₂, Pd1-TiO₂, Pd2-TiO₂, Pd3-TiO₂, and Pd4-TiO₂ aerogels after annealing.

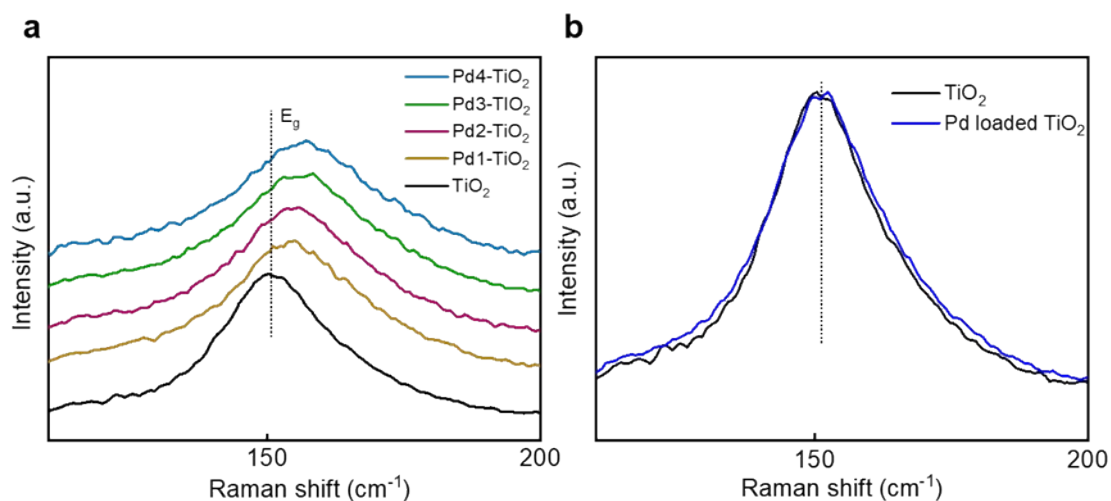


Figure S6. E_g band in the Raman spectra of (a) TiO₂, Pd1-TiO₂, Pd2-TiO₂, Pd3-TiO₂, and Pd4-TiO₂ aerogels after annealing and (b) TiO₂ and Pd loaded TiO₂ aerogels after annealing.

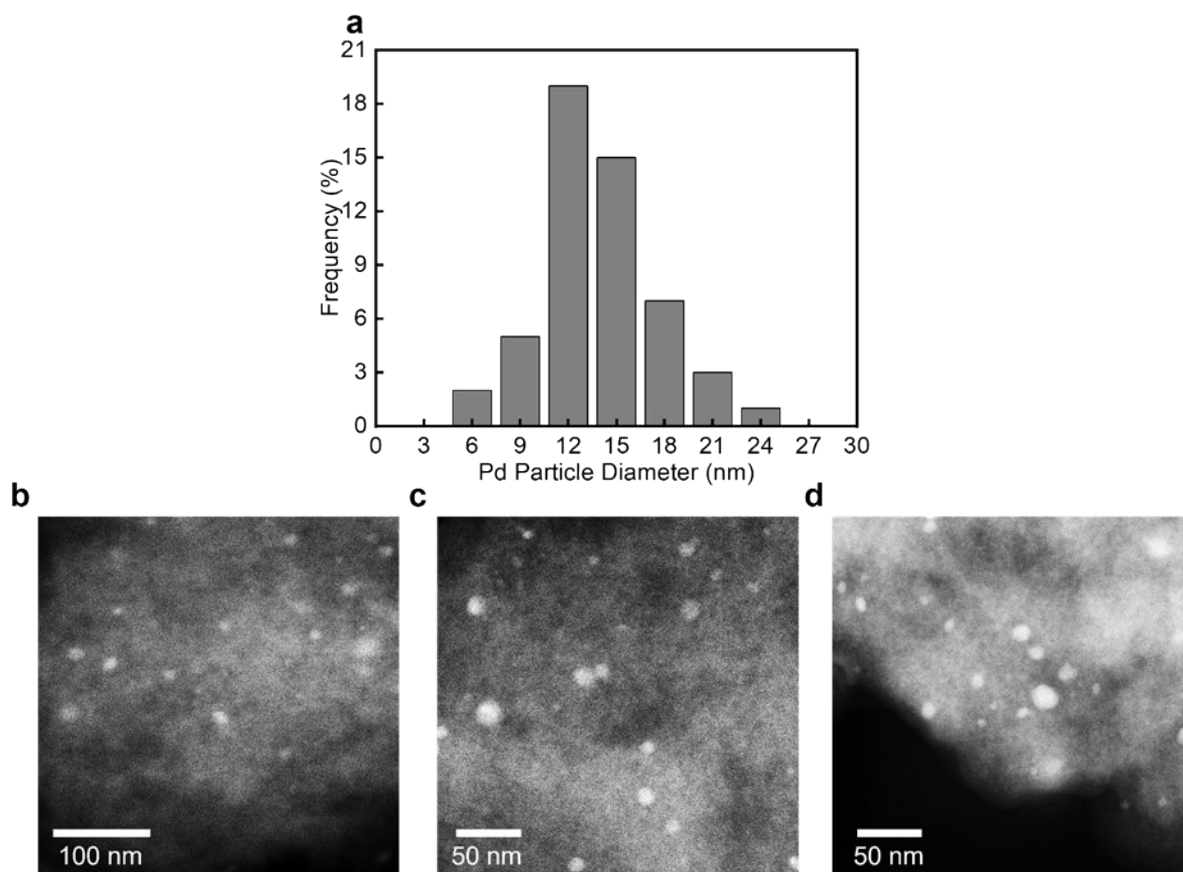


Figure S7. (a) Particle size distribution of the Pd nanoparticles in a Pd₂-TiO₂ aerogel after annealing and calculated from (b-d) STEM data.

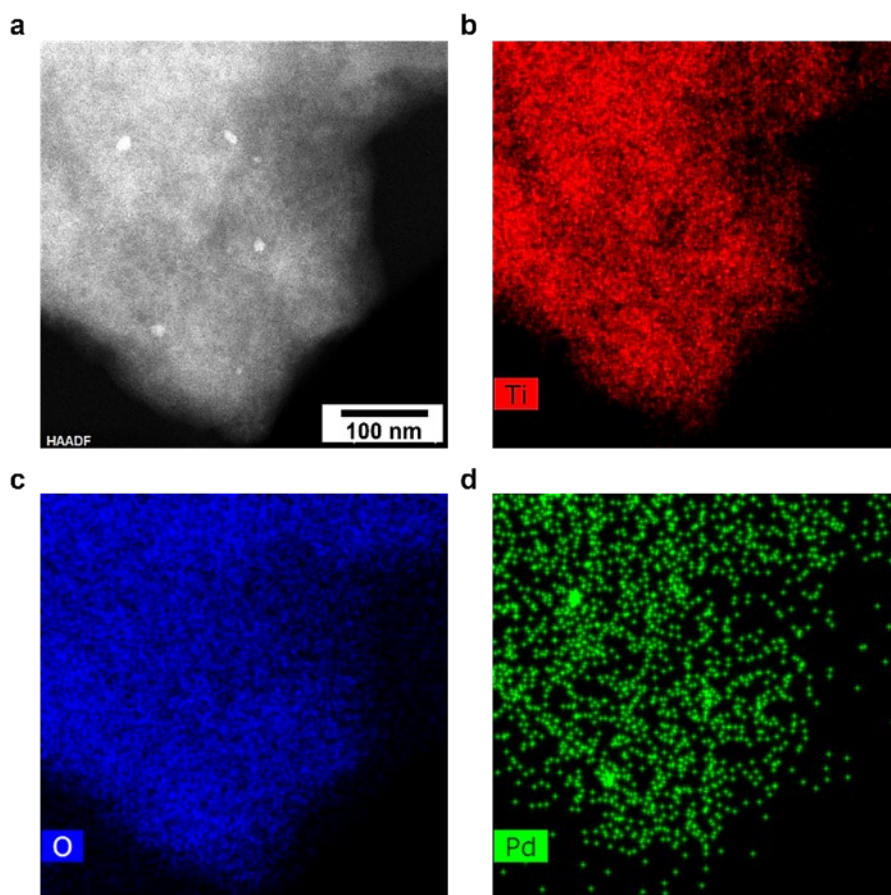


Figure S8. (a) HAADF-STEM image (a) of a Pd₂-TiO₂ aerogel with the corresponding elemental maps of (b) Ti (c) O, and (d) Pd.

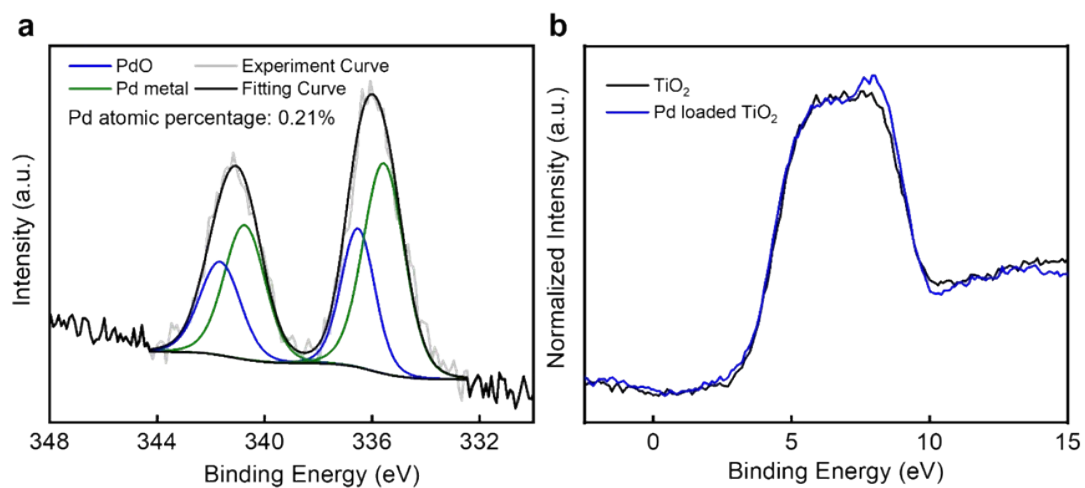


Figure S9. (a) XPS Pd 3d spectrum of a Pd loaded TiO₂ aerogel. (b) XPS valence band spectra of TiO₂ and Pd loaded TiO₂ aerogels.

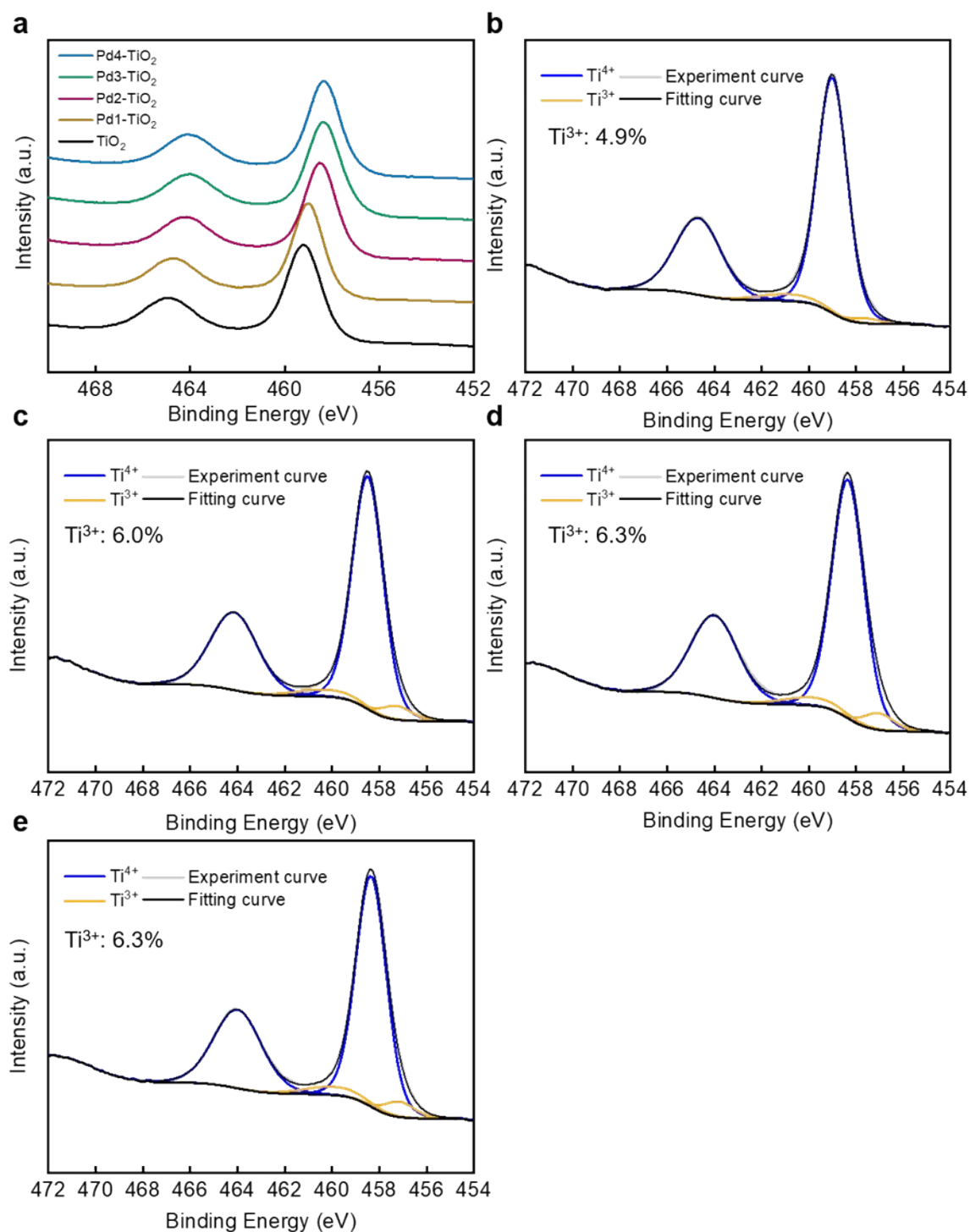


Figure S10. (a) XPS Ti 2p spectra of TiO₂, Pd1-TiO₂, Pd2-TiO₂, Pd3-TiO₂, and Pd4-TiO₂ aerogels. XPS Ti 2p spectrum of (b) Pd1-TiO₂, (c) Pd2-TiO₂, (d) Pd3-TiO₂, and (e) Pd4-TiO₂ aerogels.

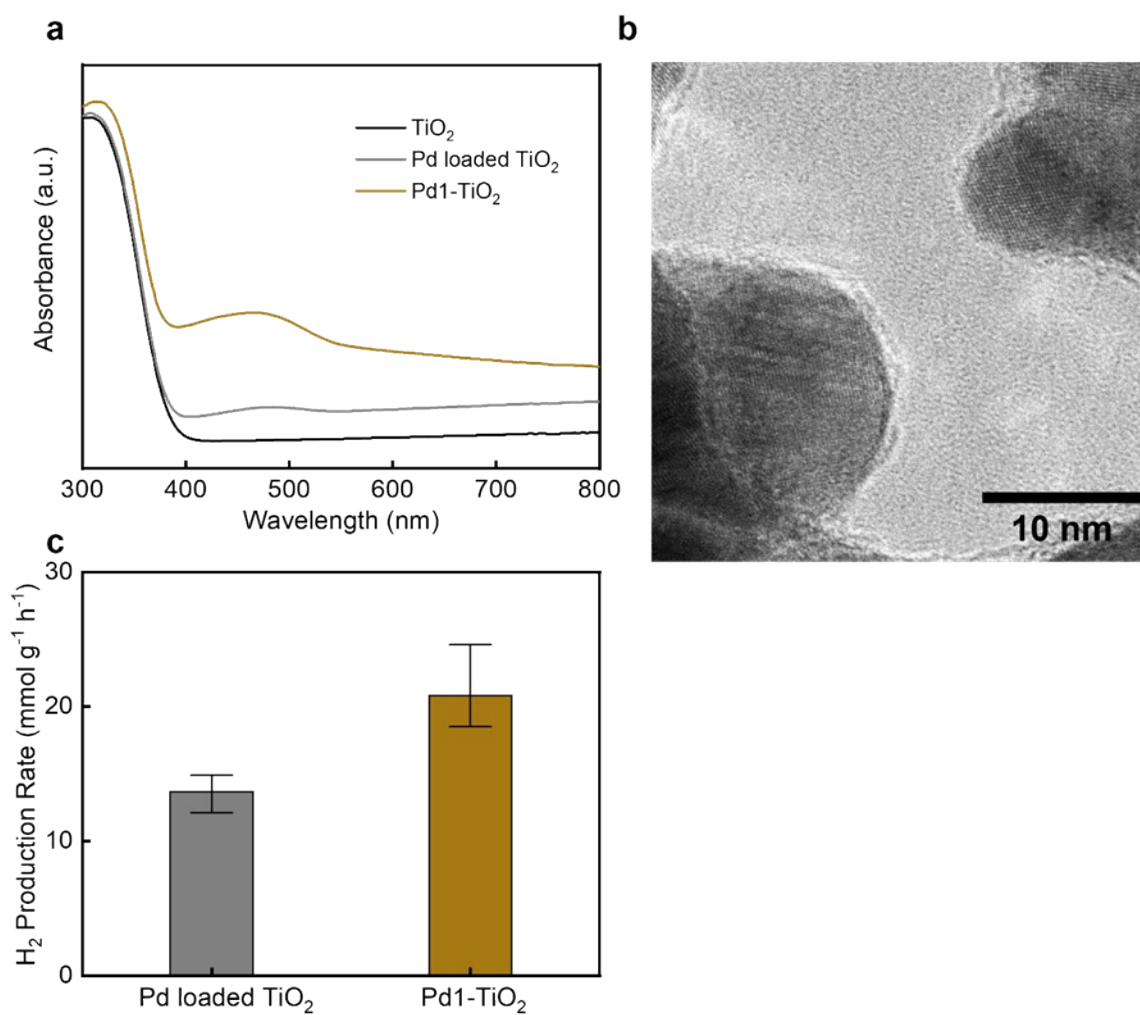


Figure S11. (a) UV-visible absorption spectra of TiO₂, Pd loaded TiO₂, and Pd1-TiO₂ aerogels. (b) HRTEM image of Pd nanoparticles used for the synthesis of a Pd loaded TiO₂ aerogel. (c) Visible light-driven photocatalytic H₂ production rates of Pd loaded TiO₂ and Pd1-TiO₂ aerogels.

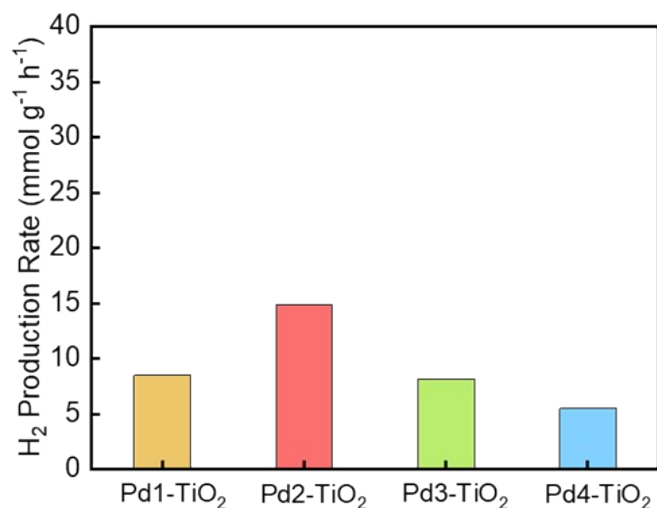


Figure S12. Visible light-driven photocatalytic H₂ production rates of Pd1-TiO₂, Pd2-TiO₂, Pd3-TiO₂, and Pd4-TiO₂ aerogels using one white LED.

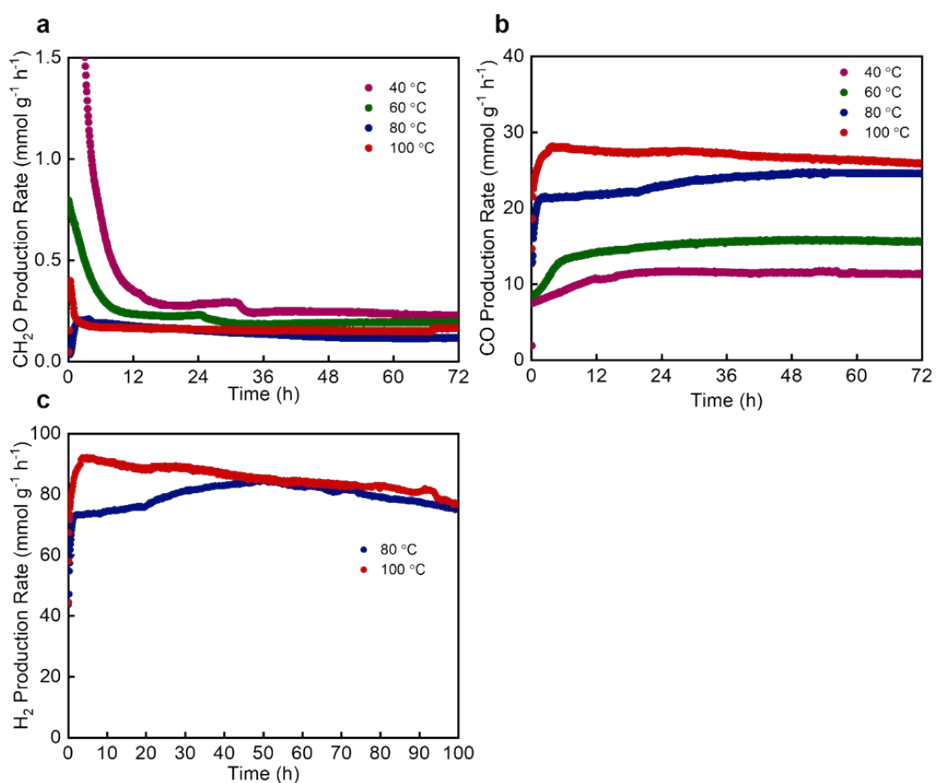


Figure S13. Production rates of (a) CH₂O and (b) CO as CH₃OH oxidation products from photocatalytic reactions using Pd2-TiO₂ aerogels at 40, 60, 80, and 100 °C. (c) Visible light-driven photocatalytic H₂ production of Pd2-TiO₂ aerogels at 80 and 100 °C for 100 h.

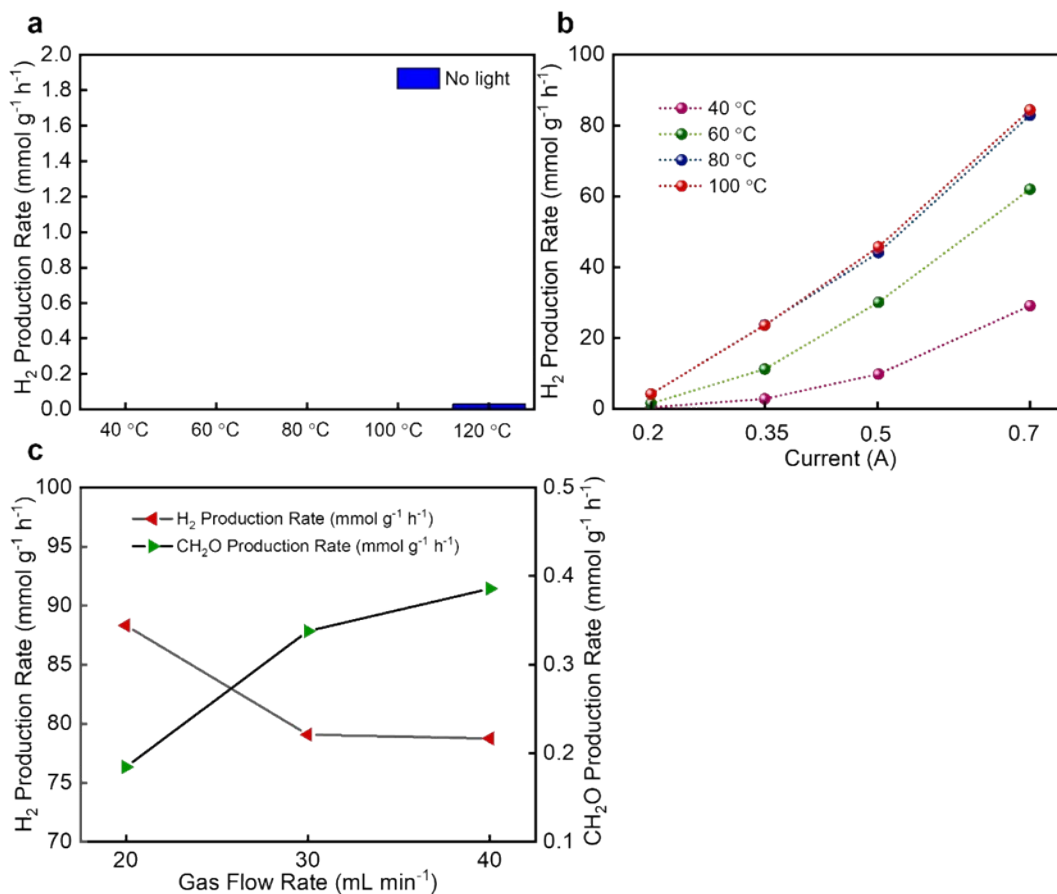


Figure S14. (a) H₂ production rates of Pd₂-TiO₂ aerogels at 40, 60, 80, 100, and 120 °C without LED illumination. (b) Photocatalytic H₂ production rates obtained with different LED intensities controlled by changing the LED currents (0.2, 0.35, 0.5, and 0.7 A). (c) H₂ and CH₂O production rates at different gas flow rates (20, 30, and 40 mL min⁻¹) under visible light.

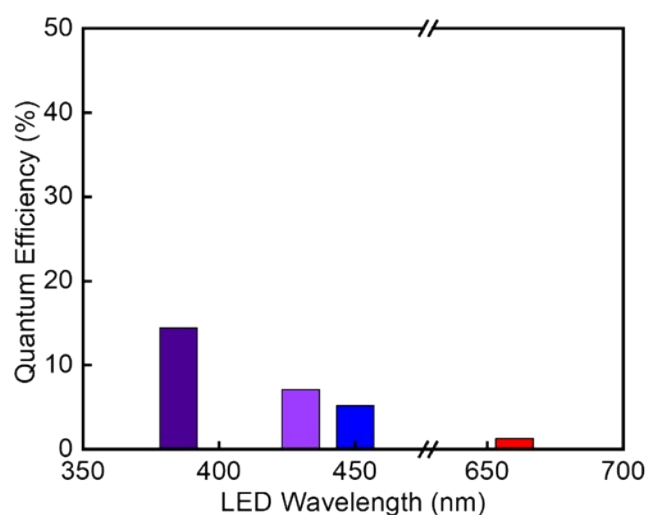


Figure S15. QE of Pd loaded TiO₂ aerogels at 100 °C under different wavelengths of LEDs.

Photocatalysts → electron (e⁻) + holes (h⁺)

CH₃OH (ad) + h⁺ → •CH₂OH (ad) + H⁺ (ad)

•CH₂OH (ad) + h⁺ → CH₂O (g) + H⁺ (ad)

CH₂O (ad) + h⁺ → •CHO (ad) + H⁺ (ad)

•CHO (ad) + h⁺ → CO (g) + H⁺ (ad)

2H⁺ (ad) + 2e⁻ → H₂ (g)

CO (ad) + H₂O (ad) → CO₂ (g) + H₂ (g)

Equation S1. Photocatalytic CH₃OH oxidation for H₂ production in a Pd modified TiO₂ aerogel.